ISSN 1392–1320 MATERIALS SCIENCE (MEDŽIAGOTYRA). Vol. 21, No. 2. 2015

Predicting Thin Film Stoichiometry in V-O_2 Reactive Sputtering

Tao WANG [1], He YU [1] *, Xiang DONG [1], Yadong JIANG [1], Roland WU [2]

[1] *School of Optoelectronic Information, University of Electronic Science and Technology of China (UESTC), Chengdu 610054, P. R. China*
[2] *Center for Plasma Material Interaction, Department of Nuclear, Plasma and Radiological Engineering, University of Illinois at Urbana-Champaign, IL, 61801, USA*

http://dx.doi.org/10.5755/j01.mm.21.2.6910

Received 09 April 2014; accepted 02 June 2014

The electrical, optical and mechanical properties of compound oxides film depend strongly on the composition of the film, especially for vanadium oxide thin films, since the vanadium-oxygen phase diagram includes mixed valence oxides with two or more oxidation states. Therefore, it is interesting to predict the film stoichiometry in VO_x films. However, it has not, to any great extent yet, been possible to predict the composition of vanadium oxides films. In this article, we present a model that enables us to predict film composition of vanadium oxides prepared by reactive sputtering. Based on this model, the fraction ratio of V, V_2O_3, VO_2 and V_2O_5 in the substrate surface as a function of oxygen flow is investigated. It is concluded that the presented theoretical model for the involved reactions and composition of VO_x thin film during reactive sputtering process is in qualitative agreement with the XPS results from experiment and can be used to find optimum processing conditions for deposition of films of a desired composition.

Keywords: vanadium oxide, film composition, reactive sputtering, theoretical model.

1. INTRODUCTION

As one of the fascinating material with excellent physical and chemical properties, vanadium oxide thin films have been studied extensively [1, 2]. VO_x films with mixture phases can be tailored to meet the demand of reasonable resistivity and relatively high temperature coefficient of resistivity (TCR), these materials have become the mainstream technology in the fast booming uncooled infrared image market. Therefore, research on the preparation techniques of VO_x thin films, has greatly been stimulated. However, the vanadium-oxygen system is a very complex compound system, because vanadium exhibits +2, +3, +4 and +5 valent states, a large number of vanadium oxides, such as VO, V_2O_3, VO_2, V_2O_5, $V_{2n}O_{5n-2}$ and V_nO_{2n-1} exist in the VO_x films. Vanadium oxides show different electronic behaviour depending on their valence configuration. The electronic and optical performance of vanadium oxide is relative to the structure of the thin films. Moreover, the reproducibility and stability of electrical properties of vanadium oxide films are dependent on the ratio of vanadium and oxygen in the film. Hence, understanding of the influence of process parameters on the film composition and microstructure is necessary. In this case, how to predict the film stoichiometry and then adjust the optical, electrical properties of the VO_x films for particular applications became a challenge.

Vanadium oxide thin films have been widely prepared by reactive magnetron sputtering method [3]. Theoretical modelling can be used as a tool to increase the understanding of this complex process. The mechanism of reactive sputtering was reasonably well described by the Berg model [4, 5], and recently the extensions to this model have been published [6 – 11]. Theoretical analysis of compounds with mixed vanadium oxide thin films have been published previously [12], however, only suboxide VO on the target was taken into consideration in the modeling and the corresponding experimental results was not given. In this paper, we assumed metal vanadium and three oxides of V_2O_3, VO_2, and V_2O_5 was formed on both target and substrate during V–O_2 reactive sputtering. Based on this assumption, more complex processes between substrate and target such as different atoms sputtered from target which dropped on substrate are involved in this model. The details are shown in the following model section. In the experimental part, we report vanadium oxide thin films deposited by magnetron sputtering method with different oxygen flows and investigate the changing fraction of V, V_2O_3, VO_2 and V_2O_5 with respect to the oxygen flow using XPS analysis.

2. MODEL

A model describing the dynamic behaviour of the reactive sputtering process for vanadium oxide has been presented previously [12]. That model takes into account vanadium metal on the target and VO_x of two different valence oxides (VO and V_2O_5) on the substrate. However, from the results of XPS measurement taken on the VO_x samples (will be seen in the experimental part), V, V_2O_3, VO_2 and V_2O_5 have been observed. The starting point of Berg's model is aimed at defining the processing conditions as correct as possible. Therefore, a new model is developed which accounts for the existence of the four states of vanadium oxides based on the experimental results. The suggested model is a further development of previously presented models.

Analogous to the earlier models, the targets are assumed to be partially covered with the compound and metal materials. The total supply rate of the reactive gas (oxygen) is denoted as Q_{tot}. In order to simulate this more

---

* Corresponding author. Tel.: +86-028-83208959. fax. +86-028-83206123.
E-mail address: *yuhe@uestc.edu.cn* (H. Yu)

efficiently, we made some additional assumptions. On one hand, the same conditions exist at the receiving area where all sputtered material is assumed to be uniformly collected.

Different from the previous model, the target surface must be divided into four parts (see Fig. 1). Here θ_{t1} is denoted as the fractional area of the target surface that consists of unreacted metal vanadium. The θ_{t2}, θ_{t3}, θ_{t4} fraction would be assumed to be covered by V_2O_3, VO_2 and V_2O_5, respectively. θ_{s1} is the fractional area of the substrate surface that consists of unreacted metal vanadium and the θ_{s2}, θ_{s3}, θ_{s4} fractions are covered by V_2O_3, VO_2 and V_2O_5, respectively.

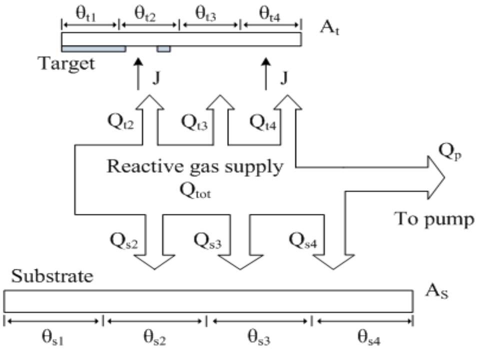

Fig. 1. Schematic of a simple reactive- sputtering system

2.1. Conditions at the target surface

Compare with the previous modelling, more simplifications must be made to keep the complexity down without losing contact with reality. For one thing, it is assumed that the gettering of reactive gas onto metal contributes to form a suboxide V_2O_3 on the substrate, increasing θ_{s2} and decreasing θ_{s1}. Further attachment (by oxygen) onto this suboxide V_2O_3 contributes to form the VO_2, thus increasing θ_{s3}, also decreasing θ_{s2}. The superoxide V_2O_5 is formed by the reaction of reactive gas and VO_2. For the other thing, additional process happened on the substrate needs to be considered. As for the metal vanadium sputtered from the target, when the metal comes from the fraction of θ_{t1} placed on the substrate surface which previously consisted of VO_x (V_2O_3, VO_2 and V_2O_5), that the fraction of θ_{s1} will increase and the fraction of $(1-\theta_{s1})$ will decrease. Furthermore, when the VO_x particle sputtered from target placed on the substrate, which previously consisted of VO_i ($i != x$), then the corresponding fraction of θ_{si} will decrease and the fraction of VO_x will increase. The fraction of flux $\frac{J}{q}Y_{ti}\theta_{ti}A_t$ deposited onto the fraction θ_{si} of the collecting area A_s will not influence the value of θ_{s1}. Adding elemental non-reacted target atoms to an area that already consist of non-reacted atoms does not change θ_{s1}.

By making the above-mentioned new assumptions in combination with the simplifications presented earlier, the balance equations for the conditions on the target should be rewritten as the following equation:

$$\frac{J}{q}Y_{t2}\theta_{t2}A_t+\frac{J}{q}Y_{t3}\theta_{t3}A_t+\frac{J}{q}Y_{t4}\theta_{t4}A_t=2\alpha_{t1}FA_t\theta_{t1}/l_2\,, \quad (1)$$

here J is the ion-current density, q is the elementary electronic charge. Y_{t2}, Y_{t3}, Y_{t4} represent the sputtering yield of the V_2O_3, VO_2 and V_2O_5. α_{t1} is the probability (sticking coefficient) for a oxygen molecule to react with a vanadium atom that comes from the θ_{t1} fraction of the target, A_t is the effective target. l_2 is the stoichiometry of the V_2O_3 taken into consider in this model, F represents neutral reactive molecules/ (unit area and time).

Eq. (1) determines the balance of the fraction of vanadium atoms (θ_{t1}) on the target. For simplicity, the sputtered material from the surface fraction $\frac{J}{q}Y_{t2}\theta_{t2}A_t+\frac{J}{q}Y_{t3}\theta_{t3}A_t+\frac{J}{q}Y_{t4}\theta_{t4}A_t$ is assumed to be sputtered as molecules, irrespective of whether the material is ejected in atomic or molecular form. The only way sputtered compound molecules may be replaced is by reactions between neutral reactive gas molecules and the elemental non-reacted vanadium atoms:

$$2\alpha_{t1}FA_t\theta_{t1}/l_2=\frac{J}{q}Y_{t2}\theta_{t2}A_t+2\alpha_{t2}FA_t\theta_{t2}/(l_3-l_2)\,, \quad (2)$$

here, α_{t2} is the sticking coefficient for the oxygen molecule to react with V_2O_3 from the fraction θ_{t2} of the target, l_3 is the stoichiometry of the VO_2.

Moreover, Eq. (2) determines the balance of the fraction of θ_{t2} on the target. The reaction between elemental target atoms and the reactive gas which takes place on the compound fraction θ_{t1} will contribute to an increase in the value of θ_{t2}. However, the compound V_2O_3 are sputtered from the surface fraction θ_{t2} that will decrease the fraction of θ_{t2}. Besides, attaching the reactive gas to V_2O_3 will contribute to a decrease in θ_{t2}:

$$2\alpha_{t2}FA_t\theta_{t2}/(l_3-l_2)=\frac{J}{q}Y_{t3}\theta_{t3}A_t+2\alpha_{t3}FA_t\theta_{t3}/(l_4-l_3)\,; \quad (3)$$

$$2\alpha_{t3}FA_t\theta_{t3}/(l_4-l_3)=\frac{J}{q}Y_{t4}\theta_{t4}A_t\,, \quad (4)$$

here, α_{t3} is the probability (sticking coefficient) for the oxygen molecule to react with VO_2 from the fraction θ_{t3} of the target, l_4 is the stoichiometry of the V_2O_5.

Similar to Eq. (2), Eq. (3) and Eq. (4) determine the balance of the fraction of θ_{t3} and θ_{t4} respectively:

$$\theta_{t1}+\theta_{t2}+\theta_{t3}+\theta_{t4}=1\,. \quad (5)$$

The expressions for θ_{t1}, θ_{t2}, θ_{t3}, θ_{t4} can be obtained by solving Eqs. (2) – (5).

2.2. Conditions at the substrate surface

At steady state, the contributions supporting an increase in θ_{si} must be identical to the contributions that support a decrease in θ_{si}. This leads to the following balance equations (Eqs. (6) through (10)) for the collecting area A_s.

Eq. (6) determines the balance of the fraction of θ_{s1} on the substrate. The fraction of flux $\frac{J}{q}Y_{t1}\theta_{t1}A_t$ deposited onto the fraction $(1-\theta_{s1})$ will increase the value of θ_{s1}. The fraction of flux $\frac{J}{q}Y_{t2}\theta_{t2}A_t+\frac{J}{q}Y_{t3}\theta_{t3}A_t+\frac{J}{q}Y_{t4}\theta_{t4}A_t$ deposited onto the fraction (θ_{s1}) will contribute to a decrease in θ_{s1}. The number of molecules which convert into V_2O_3 by oxygen is denoted by $2\alpha_{s1}FA_s\theta_{s1}/l_2$. The reaction between elemental non-reacted atoms and reactive gas will decrease the value of θ_{s1}:

$$\begin{aligned}&\frac{J}{q}Y_{t1}\theta_{t1}A_t(1-\theta_{s1}) = \\ &= (\frac{J}{q}Y_{t2}\theta_{t2}A_t + \frac{J}{q}Y_{t3}\theta_{t3}A_t + \frac{J}{q}Y_{t4}\theta_{t4}A_t)\theta_{s1} + 2\alpha_{s1}FA_s\theta_{s1}/l_2\end{aligned} \quad ,(6)$$

here α_{s1} is the sticking coefficient for the oxygen molecule to react with vanadium atom on the substrate.

$$\begin{aligned}&\frac{J}{q}Y_{t2}\theta_{t2}A_t(1-\theta_{s2}) + 2\alpha_{s1}FA_s\theta_{s1}/l_2 = \\ &= (\frac{J}{q}Y_{t1}\theta_{t1}A_t + \frac{J}{q}Y_{t3}\theta_{t3}A_t + \frac{J}{q}Y_{t4}\theta_{t4}A_t)\theta_{s2} + \quad , \\ &+ 2\alpha_{s2}FA_s\theta_{s2}/(l_3 - l_2)\end{aligned} \tag{7}$$

α_{s2} is the sticking coefficient for the oxygen molecule to react with V_2O_3 on the substrate.

Eq. (7) determines the balance of the fraction of θ_{s2} on the substrate. The fraction of flux $\frac{J}{q}Y_{t2}\theta_{t2}A_t$ deposited onto the fraction (1–θ_{s2}) will increase the value of θ_{s2}. Besides, the reaction between elemental non-reacted atoms and reactive gas will increase the value of θ_{s2}. However, the fraction of flux $\frac{J}{q}Y_{t1}\theta_{t1}A_t + \frac{J}{q}Y_{t3}\theta_{t3}A_t + \frac{J}{q}Y_{t4}\theta_{t4}A_t$ deposited onto the fraction (θ_{s2}) will contribute to a decrease in θ_{s2}. The flux $2\alpha_{s2}FA_s\theta_{s2}/(l_3 - l_2)$ consumed by the reaction between compound V_2O_3 and reactive gas will decrease the value of θ_{s2}:

$$\begin{aligned}&\frac{J}{q}Y_{t3}\theta_{t3}A_t(1-\theta_{s3}) + 2\alpha_{s2}FA_s\theta_{s2}/(l_3 - l_2) = \\ &= (\frac{J}{q}Y_{t1}\theta_{t1}A_t + \frac{J}{q}Y_{t2}\theta_{t2}A_t + \frac{J}{q}Y_{t4}\theta_{t4}A_t)\theta_{s3} + , \\ &+ 2\alpha_{s3}FA_s\theta_{s3}/(l_4 - l_3)\end{aligned} \tag{8}$$

α_{s3} is the sticking coefficient for the oxygen molecule to react with VO_2 on the substrate.

Eq. (8) determines the balance of the fraction of θ_{s3} on the substrate. The fraction of flux $\frac{J}{q}Y_{t3}\theta_{t3}A_t$ deposited onto the fraction (1–θ_{s3}) will increase the value of θ_{s3}. Besides, the reaction between compound V_2O_3 and reactive gas will increase the value of θ_{s3}. However, the fraction of flux $(\frac{J}{q}Y_{t1}\theta_{t1}A_t + \frac{J}{q}Y_{t2}\theta_{t2}A_t + \frac{J}{q}Y_{t4}\theta_{t4}A_t)\theta_{s3}$ deposited onto the fraction (θ_{s2}) will contribute to a decrease in θ_{s2}. Moreover, the flux $2\alpha_{s3}FA_s\theta_{s3}/(l_4 - l_3)$ consumed by the reaction between compound VO_2 and reactive gas will decrease the value of θ_{s3}.

Similar to the above discussion, a steady-state equation for the fraction of V_2O_5 on the substrate may therefore be defined as:

$$\begin{aligned}&\frac{J}{q}Y_{t4}\theta_{t4}A_t(1-\theta_{s4}) + 2\alpha_{s3}FA_s\theta_{s3}/(l_4 - l_3) = \\ &= (\frac{J}{q}Y_{t1}\theta_{t1}A_t + \frac{J}{q}Y_{t2}\theta_{t2}A_t + \frac{J}{q}Y_{t4}\theta_{t4}A_t)\theta_{s4}\end{aligned} \quad . \tag{9}$$

Finally, the sum of fractions (θ_{s1}, θ_{s2}, θ_{s3}, θ_{s4}) is equal to 1:

$$\theta_{s1} + \theta_{s2} + \theta_{s3} + \theta_{s4} = 1 . \tag{10}$$

2.3. Gettering of the reactive gas

Compound formation by reaction between reactive gas molecules and elemental non-reacted atoms, compound V_2O_3, compound VO_2 at the target will consume reactive gas molecules Q_{t1}, Q_{t2}, Q_{t3} reactively. Thus, the consumption (number of oxygen molecules per unit time) at the target Q_t can be obtained from Eq. (11):

$$\begin{aligned}&Q_{t1} = 2\alpha_{t1}FA_t\theta_{t1}/l_2 ; \\ &Q_{t2} = 2\alpha_{t2}FA_t\theta_{t2}/(l_3 - l_2) ; \\ &Q_{t3} = 2\alpha_{t3}FA_t\theta_{t3}/(l_4 - l_3) ; \\ &Q_t = Q_{t1} + Q_{t2} + Q_{t3} .\end{aligned} \tag{11}$$

While the consumption Q_s at the collecting area A_s can be expressed by Eq. (12):

$$\begin{aligned}&Q_{s1} = 2\alpha_{s1}FA_s\theta_{s1}/l_2 ; \\ &Q_{s2} = 2\alpha_{s2}FA_s\theta_{s2}/(l_3 - l_2) ; \\ &Q_{s3} = 2\alpha_{s3}FA_s\theta_{s3}/(l_4 - l_3) ; \\ &Q_s = Q_{s1} + Q_{s2} + Q_{s3} .\end{aligned} \tag{12}$$

Here, Q_{s1} is reactive gas molecules consumed by reactive gas oxygen molecules and non-reacted vanadium atoms at collecting area. Q_{s2} is reactive gas molecules consumed by oxygen and V_2O_3 compound. The other part Q_{s3} is reactive gas molecules consumed by oxygen and VO_2 compound.

The remaining part Q_p of the reactive gas will escape from the processing chamber through the pumping system:

$$Q_p = \frac{PN_a}{R_r T} S \, , \tag{13}$$

here, P is the partial pressure of oxygen, N_a is Avogadro constant, R_r is general gas constant, T is the temperature, S is the pumping speed.

Eqs. (1) through (5) describe the conditions at the target, in conjunction with Eqs. (6) through (10), make up a set of equations that can be easily solved by a computer.

The total supply rate of the reactive gas is denoted Q_{tot}:

$$Q_{tot} = Q_t + Q_s + Q_p . \tag{14}$$

3. EXPERIMENTAL

VO_x thin films were deposited by DC reactive magnetron sputtering in a custom-built vacuum system, as shown in Fig. 2. A water cooled rectangle planar vanadium metal target, with the purity level of 99.99 %, was used in these experiments. The deposition chamber was evacuated to a base pressure of about 1.0×10^{-4} Pa by combining turbomolecular and rotary vane pumps. Argon and oxygen flow were controlled by using independent mass flow controllers, the argon flow was kept constant at 100 sccm and the oxygen flow was varied from 1.0 sccm to 6.0 sccm. Glass slides were used as substrates. Before the substrates were mounted on a substrate holder, they were ultrasonically cleaned in acetone, ethanol and de-ionized water for 20 min sequentially, and then dried by pure nitrogen stream. For all the experiments, two steps were applied: cleaning of the vanadium target surface by pre-sputtering of 15 min in a pure argon atmosphere, followed by reactive deposition of VO_x films for around 25 min. The substrate holder was rotated at 10 rpm to ensure uniformity of film deposition and there were no intentionally heating during experiment. So the deposition temperature is 300 K.

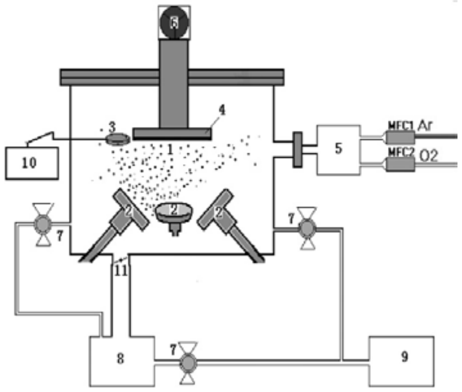

Fig. 2. Reactive sputter deposition system (1) substrate (2) magnetron sources (3) quartz microbalance (4) resistive heater (5) gas supply (6) rotating controller (7) small angle valves (8) turbo pump (9) rotary pump (10) frequency meter (11) slide valve

X-ray photoelectron spectroscopy (XPS) spectra were taken by using XSAM800 system (Kratos Ltd., Al Kα X-ray source without monochromatization, the base pressure of the ultrahigh vacuum chamber was lower than 3×10^{-7} Pa, binding energies (BE) were determined using C1s peak at 284.8 eV as a reference, the resolution is 0.9 eV/10^4 counts per second).

4. RESULTS AND DISCUSSION

The influence of the oxygen flow rate on the stoichiometry of the deposited vanadium oxide was examined by the X-ray photoemission spectroscopy (XPS). To avoid surface effects, like contamination, the XPS spectra were taken in the depth of the samples after preliminary sputtering.

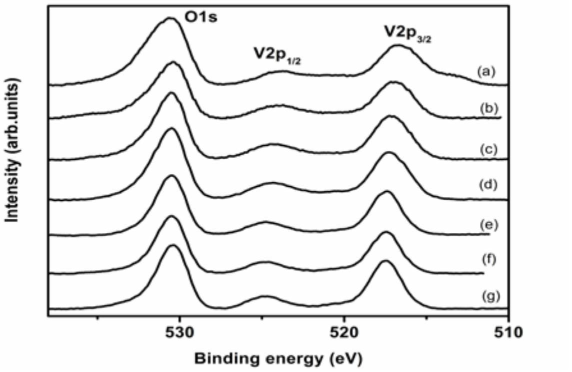

Fig. 3. XPS spectra of the V 2p and O 1s region of films. Oxygen flow is: a – 1 sccm; b – 3 sccm; c – 3.8 sccm; d – 4.2 sccm; e – 4.4 sccm; f – 4.6 sccm; g – 6 sccm

Fig. 3 shows the XP spectra of the O 1s and V 2p core level emission lines taken at different samples with varied oxygen flow. Spectra (a – g) show that the V $2p_{3/2}$ and V $2p_{1/2}$ lines become narrower and shift to higher binding energies with increasing oxygen flow, suggesting more vanadium fractions with higher oxidation states existed in the film. In order to analyze this process in more detail, the background corrected XPS spectra of the V $2p_{3/2}$ lines was fitted with mixed Lorentzian-Gaussian [13] profiles after subtraction of a Shirley function [14 – 15] using software XPSpeak4.1. In Fig. 4, the lines in different colours centred at 512.6, 515.1, 516.2 and 517.2 eV show presence of different components. Comparison of these values with the data found in the literature [16 – 20] allows attributing these components to V, V^{3+}, V^{4+}, and V^{5+} oxidation states of vanadium, respectively.

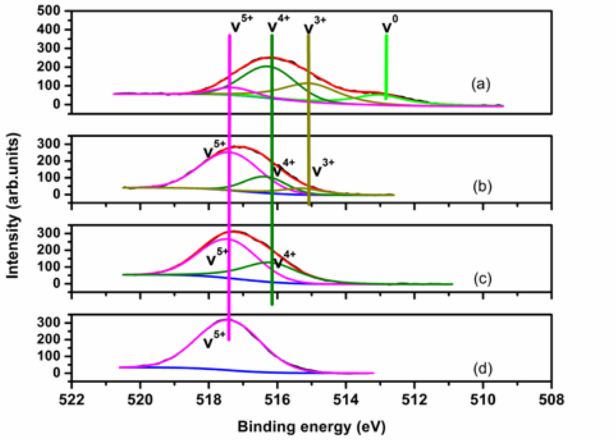

Fig. 4. V $2p_{3/2}$ lines of vanadium oxides film taken at different samples with different oxygen flow. Oxygen flow is: a – 1 sccm; b – 4.2 sccm; c – 4.4 sccm; d – 6 sccm

When the oxygen flow is fairly low (spectrum (a)), all the four species state was found. With increasing oxygen flow (spectrum (b)), V^0 species disappear gradually which is due to the higher oxygen concentration. When oxygen flow is increased to around 4.4 sccm, the intensity of V^{3+} species is removed. At high oxygen flow (spectrum (d)), only V^{5+} species are existed.

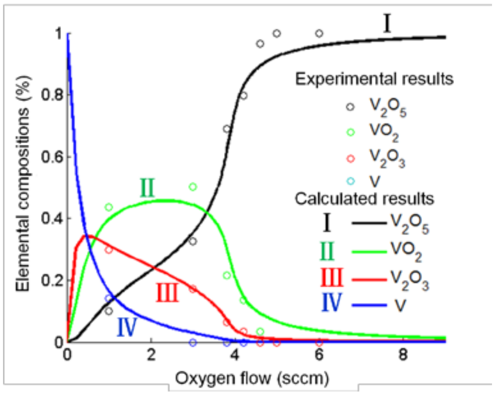

Fig. 5. Experimental results and simulations of the elemental compositions (V, V_2O_3, VO_2, and V_2O_5) vs. different oxygen flow

It is possible to combine Eqs. (1) through (14) and solve all the fractions of target and substrate vs. reactive gas flow Q_{tot}. From the simulation results obtained, the substrate surface coverage has been estimated. The elemental compositions versus oxygen flows from these experiments and simulations are shown in Fig. 5. It is seen that θ_{s1}, corresponding to the fractional area of the substrate consisting of metal vanadium, decreases most rapidly for low reactive gas flows, but decreases asymptotically to zero for high flows. In the region up to 3.5 sccm, the fraction of θ_{s4} is higher than θ_{s3} and θ_{s1} reaches almost zero. Furthermore, with the continued increasing amount of oxygen, θ_{s4} increases asymptotically to one. Meanwhile, the fraction of metal V, V_2O_3 and VO_2 is reduced and eventually disappeared. It is seen that the trends in the experiments are adequately described by the simulations. There are several reasons to explain these curves. For zero flow of oxygen, the target is to some extent oxidized and the rest is metallic, while at higher flows of oxygen, target is essentially oxidized. After the 3.5 sccm point, the amount of O_2 consumed to VO_2 surpassed the amount of O_2 gettered by deposited V and V_2O_3, resulting in a drastic increase in the fraction of θ_{s4}. It should also be noted that the content of V_2O_3 decreases from around 35 % to approximately 10 % in the region from 0.6 sccm to 3.8 sccm while the content of VO_2 is somewhat increased from 35 % to 42 %. This means that the films contain significantly more VO_2 than V_2O_3. This is a consequence of the higher reactivity of V_2O_3 than V with oxygen. However, even though the trends are correctly reproduced in the simulations, there are discrepancies between the experiments and simulations. The content of VO_2 and V_2O_5 for experiments is somewhat higher while the content of metal V is somewhat lower than that of simulations. There are several factors contributing to the discrepancies in simulation results with respect to the experimental results. Unfortunately, it is not possible to sort out the effects in order of their impact. It assumed in the simulations that the content of metal V was 100 % for zero flow of oxygen, but the target is usually to some extent oxidized initially. Moreover, there might be pressure gradients in the system that is not considered in the simulations. Another error is from XPS analysis.

5. CONCLUSION

A kinetic model of reactive sputtering is proposed to modify Berg's model by taking into account the four species state of V, V_2O_3, VO_2, and V_2O_5 in the vanadium oxides film. The fraction of compound on the substrate has been investigated as a function of reactive gas flow during the reactive sputtering of multicomponent thin film. From the results of simulation, substrate surface coverage has been estimated. Vanadium oxide films have been deposited by reactive magnetron sputtering using a constant current and varying the oxygen flow. Film compositions obtained from the XPS analysis were compared to the composition obtained from simulations and the agreement is satisfactory. The results from modeling are compared with the corresponding experimental results. The model can be used to find optimum processing conditions for deposition of films of a desired VO_x composition.

Acknowledgments

This work was partially supported by the National Science Foundation of China (NSFC) Grant Nos. 61405027, 61421002 and Postdoctoral Science Foundation of China (Grant No. 2014M562296).

APPENDIX A

The following simulation parameters were used in the work: $\alpha_{t1} = 0.95$, $\alpha_{t2} = 0.95$, $\alpha_{t3} = 0.95$, $\alpha_{s1} = 1$, $\alpha_{s2} = 1$, $\alpha_{s3} = 1$, $Y_{t1} = 0.6$, $Y_{t2} = 0.3$, $Y_{t3} = 0.2$, $Y_{t4} = 0.2$. Target area $A_t = 260\ \text{cm}^2$, gas temperature $T = 300$ K, pumping speed $S = 0.2\ \text{m}^3/\text{s}$.

REFERENCES

1. **Kucharczyk, D., Niklewski, T.** Accurate X-ray Determination of the Lattice Parameters and the Thermal Expansion Coefficients of VO_2 Near the Transition Temperature *Journal of Applied Crystallography* 12 1979: pp. 370 – 373.
2. **Wei, X., Zhi, M., Xu, X., Wang, T., Tang, J., Li, W., Jiang, Y.** Growth Mode and Texture Study in Vanadium Dioxide Thin Films Deposited by Magnetron Sputtering *Journal of Physics D-Applied Physics* 41 2008: pp. 055303.
3. **Schlag, H. J., Scherber, W.** New Sputter Process for VO_2 Thin Films and Examination with MIS-elements and C-V-Measurements *Thin Solid Films* 366 (1) 2000: pp. 28 – 31. http://dx.doi.org/10.1016/S0040-6090(00)00711-2
4. **Berg, S., Nyberg, T.** Fundamental Understanding and Modeling of Reactive Sputtering Processes *Thin Solid Films* 476 2005: pp. 215 – 230.
5. **Jonsson, L. B., Nyberg, T., Berg, S.** Dynamic Simulations of Pulsed Reactive Sputtering Processes *Journal of Vacuum Science & Technology A* 18 (2) 2000: pp. 503 – 508.
6. **Strijckmans, K., Leroy, W. P., Gryse, R., Depla, D.** Modeling Reactive Magnetron Sputtering: Fixing the Parameter Set *Surface & Coating Technology* 206 2012: pp. 3666 – 3675. http://dx.doi.org/10.1016/j.surfcoat.2012.03.019
7. **Depla, D., Heirwegh, S., Mahieu, S., Haemers, J., Gryse, R. D.** Understanding the Discharge Voltage Behavior during Reactive Sputtering of Oxides *Journal of Applied Physics* 101 2007: pp. 013301.
8. **Sarhammar, E., Strijckmans, K., Nyberg, T., Steenberge, S., Berg, S., Depla, D.** A Study of the Process Pressure Influence in Reactive Sputtering Aiming at Hysteresis Elimination *Surface & Coating Technology* 232 2013: pp. 357 – 361.
9. **Kubart, T., Depla, D., Martin, D. M., Nyberg, T., Berg, S.** High Rate Reactive Magnetron Sputter Deposition of Titanium Oxide *Applied Physics Letters* 92 2008: pp. 221501.
10. **Kubart, T., Jensen, J., Nyberg, T., Lijeholm, L., Depla, D., Berg, S.** Influence of the Target Composition on Reactively Sputtered Titanium Oxide *Vacuum* 83 (10) 2009: pp. 1295 – 1298.
11. **Kubart, T., Trinh, D. H., Lijeholm, L., Hultman, L., Berg, S.** Experiments and Modeling of Dual Reactive Magnetron Sputtering Using Two Reactive Gases *Journal of Vacuum Science & Technology A* 26 (4) 2008: pp. 565 – 570.
12. **Yu, H., Jiang, Y., Wang, T., Wu, Z., Yu, J., Wei, X.** Modeling for Calculation of Vanadium Oxide Film Composition in Reactive Sputtering Process *Journal of Vacuum Science & Technology A* 28 (3) 2010: pp. 466 – 471.
13. **Silversmit, G., Depla, D., Poelman, H., Marin, G., Gryse, R.** Determination of the V2p XPS Binding Energies for Different Vanadium Oxidation States (V^{5+} to V^{0+}) *Journal Electron Spectroscopy Related Phenomena* 135 (2) 2004: pp. 167 – 175. http://dx.doi.org/10.1016/j.elspec.2004.03.004
14. **Benayad, A., Martinez, H., Gies, A., Pecquenard, B., Levasseur, A., Gonbeau, D.** XPS Investigations Achieved on the First Cycle of V_2O_5 Thin Films Used in Lithium Microbatteries *Electron Spectroscopy Related Phenomena* 150 (1) 2006: pp. 1 – 10.
15. **Shi, Q., Huang, W., Xu, Y., Zhang, Y., Yue, F., Qiao, S., Zheng, S., Yan, J.** Synthesis and Terahertz Transmission Properties of Nano-porous Vanadium Dioxide Films *Journal of Physics D-Applied Physics* 45 2012: pp. 385302.
16. **Della, M., Sambi, M., Granozzi, G.** Ultrathin $VO_x/TiO_2(110)$ Film Preparation by Controlled Oxidation of Metal Deposits *Surface Science* 436 1999: pp. 227 – 236.
17. **Petukhov, M., Andrea, G., Granozzi, G.** Ultrathin Film Growth and Spectroscopic Characterization of VO_x on Pt(1 1 1). *Surface Science* 490 (3) 2001: pp. 376 – 384. http://dx.doi.org/10.1016/S0039-6028(01)01356-5
18. **Sawatzky, G., Post, D.** X-ray Photoelectron and Auger Spectroscopy Study of Some Vanadium Oxides *Physics Review B* 20 (4) 1979: pp. 1546 – 1555.
19. **Mendialdua, J., Casanova, R., Barbaux, Y.** XPS Studies of V_2O_5, V_6O_{13}, VO_2 and V_2O_3 *Electron Spectroscopy Related Phenomena* 71 (3) 1995: pp. 249 – 261.
20. **Demeter, M., Neumann, M., Reichelt, W.** Mixed-valence Vanadium Oxides Studied by XPS *Surface Science* 454 (20) 2000: pp. 41 – 44. http://dx.doi.org/10.1016/S0039-6028(00)00111-4